PAPER

Check for updates

TiO$_2$-decorated porous carbon nanofiber interlayer for Li–S batteries

Meltem Yanilmaz [ID]

Lithium–sulfur (Li–S) batteries are the most promising energy storage systems owing to their high energy density. However, shuttling of polysulfides detracts the electrochemical performance of Li–S batteries and thus prevents the commercialization of Li–S batteries. Here, TiO$_2$@porous carbon nanofibers (TiO$_2$@PCNFs) are fabricated *via* combining electrospinning and electrospraying techniques and the resultant TiO$_2$@PCNFs are evaluated for use as an interlayer in Li–S batteries. TiO$_2$ nanoparticles on PCNFs are observed from SEM and TEM images. A high initial discharge capacity of 1510 mA h g^{-1} is achieved owing to the novel approach of electrospinning the carbon precursor and electrospraying TiO$_2$ nanoparticles simultaneously. In this approach TiO$_2$ nanoparticles capture polysulfides with strong interaction and the PCNFs with high conductivity recycle and re-use the adsorbed polysulfides, thus leading to high reversible capacity and stable cycling performance. A high reversible capacity of 967 mA h g^{-1} is reached after 200 cycles at 0.2C. The cell with the TiO$_2$@PCNF interlayer also delivers a reversible capacity of around 1100 mA h g^{-1} at 1C, while the cell without the interlayer exhibits a lower capacity of 400 mA h g^{-1}. Therefore, this work presents a novel approach for designing interlayer materials with exceptional electrochemical performance for high performance Li–S batteries.

1. Introduction

Energy storage and conversion devices will play a critical role in the future as the fossil energy sources are diminishing.[1,2] Lithium ion batteries have been widely used in many portable electronics and electric vehicles however safety is still an issue for lithium ion batteries.[3,4] Lithium–sulfur batteries are attracting great interest due to ever-increasing demand for high capacity batteries. Sulfur has a high theoretical capacity of 1675 mA h g^{-1} with an operating voltage of 2.1 V. Furthermore, it is an environmentally friendly and naturally abundant material. However, the inherent poor conductivity, large volume chance of sulfur and shuttle effect deteriorate the electrochemical performance and prevent commercialization of Li–S batteries.[4–9]

Several attempts have been reported including hollow TiO$_2$-webbed carbon nanotubes,[10] MXene nanosheets decorated with TiO$_2$ quantum dots,[11] hollow porous titanium nitride tubes,[12] CoS @rGO,[13] CNT/graphene–Li$_2$S aerogel[14] to improve electrochemical performance of Li–S batteries. However, introducing carbon in sulfur cathode leads to lower energy density and the complicated and high-cost methods are not suitable for scaling up.[5,15] An atomic-scale electrocatalyst was reported to expedite the sulfur redox reactions in Li–S batteries by Li *et al.*[8] and significant improvement in electrochemical performance was achieved. Lei *et al.*[16] coated a thin layer of reduced graphene oxide/sodium lignosulfonate composite on the standard polypropylene separator and a highly robust battery with a capacity retention of 74% over 1000 cycles was reported. In another study, polyacrylonitrile and ammonium polyphosphate were electrospun into a multifunctional separator for stable and safe Li–S batteries.[17] Chen *et al.*[18] reported atomic interlamellar ion path lithiummontmorillonite for high sulfur content Li–S battery and high rate stable cycling performance was observed. Polyisoprene@sulfur in interlayers of Ti$_3$C$_2$T$_x$ was reported as a novel structure to regulate the nucleation and heterogeneous growth of Li$_2$S to prevent arbitrary Li$_2$S accumulation on host surface.[19]

Inserting porous and conductive carbon interlayer between the cathode and separator has been reported to improve the conductivity of cathode and trap lithium polysulfides. Up to day, carbonized cellulose paper,[20] carbon paper,[21] carbonized filter paper,[22] microporous carbon paper,[23] carbon fiber cloth[24] were reported, however, the improvement is not satisfactory due to low interaction between carbon and polysulfides. Thicker carbon layer is certainly more effective to physically absorb polysulfides however, it slows down ion movement and lowers volumetric energy density of the cells.[15,25]

It has been reported that metal oxides (TiO$_2$, MnO$_2$, and MgO, V$_2$O$_5$ *etc.*) and sulfides (MoS$_2$, TiS$_2$, VS$_2$, *etc.*) have strong adsorption for the polysulfides, because of the intense electrostatic attraction between metal–oxygen bond and polysulfides. TiO$_2$ also has the low cost advantage.[5,6,15,26] In this work,

Department of Textile Engineering, Istanbul Technical University, Istanbul, Turkey. E-mail: yanilmaz@itu.edu.tr

electrospinning and electrospraying techniques were utilized simultaneously, for the first time, to fabricate interlayer materials for Li–S batteries. PAN/PMMA blend solution was electrospun while TiO_2 dispersion in methanol was electrosprayed at the same time. Then, TiO_2@PCNFs were obtained after the heat treatment in which PAN turned into carbon and PMMA generated pores. The obtained fibrous mat was directly used as an interlayer between the separator and the cathode in Li–S cells. In TiO_2@PCNF interlayer, PCNF layer promotes electron transfer and TiO_2 plays a vital role in entrapment of polysulfides *via* strong chemical interaction. The high initial capacity of 1510 mA h g^{-1} and the reversible capacity of 967 mA h g^{-1} were observed after 200 cycles from the cell with TiO_2@PCNF interlayer, whereas the cell prepared with PCNF interlayer delivered initial capacity of 1326 mA h g^{-1} and reversible capacity of 500 mA h g^{-1} after 200 cycles. The cell prepared without interlayer only delivered initial capacity of 967 mA h g^{-1} and reversible capacity of 206 mA h g^{-1}. The cell resistance and C-rate performance was also improved with conductive nanostructured carbon layer decorated with TiO_2. Therefore, this work demonstrate that employing TiO_2 decorated PCNF interlayer *via* electrospinning and electrospraying could be very effective approach to fabricate high performance Li–S batteries.

2. Experimental

Polyacrylonitrile (PAN, M_w = 150 000), polymethylmethacrylate (PMMA, M_w = 200 000) and *N,N*-dimethyl formamide (DMF), sulfur (99%), methanol, 1,3-dioxolane, 1,2 dimethoxyethane, bis(trifluoromethane), sulfonamide lithium, lithium nitrite, *N*-methyl-2-pyrrolidone were supplied from Sigma Aldrich. Polyvinylidene fluoride (PVDF, Solef 5130) and TiO_2 with D30 nm were supplied from Solvay and SSNanomaterials, respectively.

12 wt% PAN/PMMA (7/3, w/w) blend solution was prepared in DMF and stirred for 24 hours at ambient temperature while TiO_2 dispersion was prepared in methanol. The PAN/PMMA solution was then electrospun into nanofibers and TiO_2 dispersion was electrosprayed simultaneously with the following process parameters: flow rate of 1 ml h^{-1}, voltage of 20 kV, and tip-to-collector distance of 20 cm. To form TiO_2@PCNFs, electrospun PAN/PMMA nanofibers decorated with TiO_2 nanoparticles were stabilized in air at 280 °C for 2.5 h with a heating rate of 5 °C min^{-1} and were carbonized at 800 °C for 2 h in argon atmosphere with a heating rate of 2 °C min^{-1}, during which PAN nanofibers were converted to carbon nanofibers and PMMA was decomposed to generate pores in the carbon matrix.

The morphology of PCNFs, TiO_2@PCNFs was investigated by JEOL SEM-7100-EDX scanning electron microscope and JEOL TEM-1400-EDX transmission electron microscope. X-ray diffraction (XRD) patterns were examined by using a diffractometer (Japan) with Cu Ka radiation (λ = 0.154 nm) in a 2θ range from 10° to 70°.

The sulfur cathode was prepared by casting a slurry containing 70 wt% pure sulfur, 20 wt% carbon and 10 wt% PVDF binder in NMP on the aluminum foil using doctor-blade technique, followed by drying in an air oven at 60 °C for 12 h. It is

punched out and precisely weighed. The electrodes with sulfur loadings between 1 mg were cut into discs of 12 mm in diameter. The electrolyte was kept constant as 40 μl per 1 mg sulfur.

The charge–discharge tests of Li–S cells were conducted by using CR 2032 coin cells. The cells were assembled in an argon filled glovebox using electrolyte consisting of 1.0 M LiTFSI in distilled DME : DOL (1 : 1, v/v), sulfur cathode, separator, Li foil anode with TiO_2@PCNF and PCNF interlayer. For comparison, the Li–S cells without interlayer was also assembled. Furthermore, electrochemical impedance spectroscopy (EIS) was employed to examine the resistance of the prepared cells in the range of 100 kHz to 0.1 Hz with 5 mV amplitude and cycling voltammetry was performed to investigate the electrochemical characteristics.

3. Results and discussion

3.1 Morphology and structure characterization

SEM images of PCNFs and TiO_2@PCNFs are shown in Fig. 1. The average nanofiber diameter was measured to be around 160 nm for PCNFs. SEM image of TiO_2@PCNFs revealed that TiO_2 nanoparticles were decorated on PCNFs. In order to further investigate the morphology of TiO_2@PCNFs, TEM images are reported in Fig. 2. TEM images also proved uniform distribution of TiO_2 nanoparticles on highly conductive carbon nanofiber interlayer which not only could buffer the volume
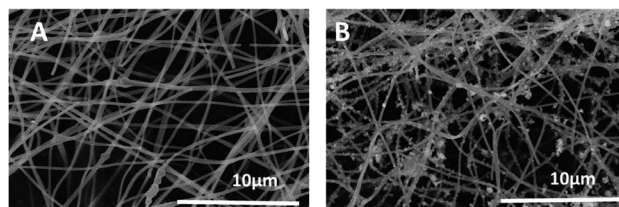

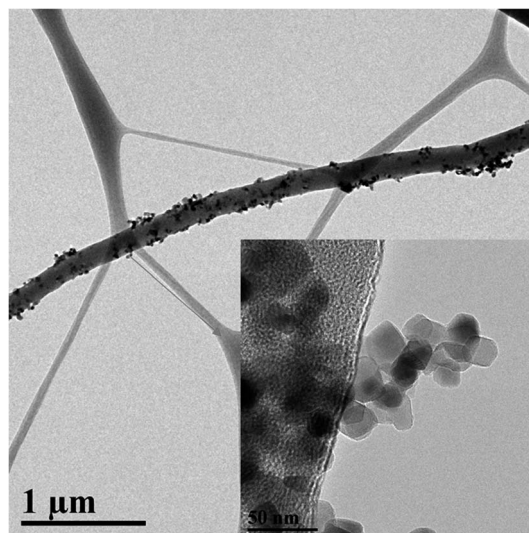**Fig. 1** SEM images of PCNFs (A), TiO_2@PCNFs (B).
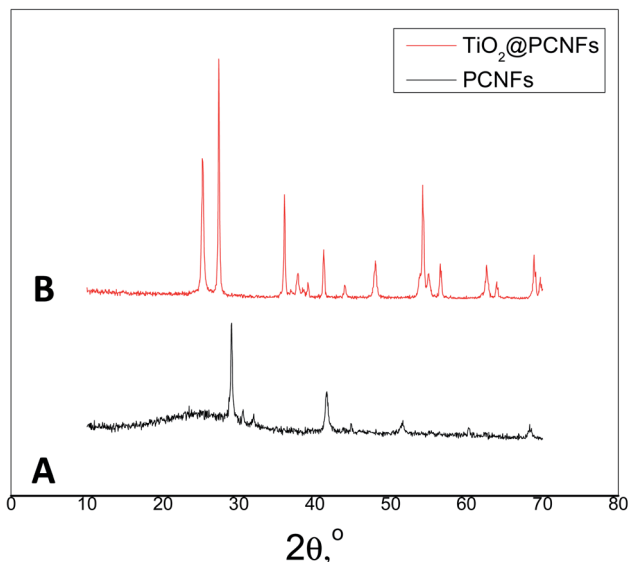

Fig. 2 TEM images of TiO_2@PCNFs.

Fig. 3 XRD patterns of PCNFs (A), TiO$_2$@PCNFs (B).

Table 1 BET measurement of PCNFs and TiO$_2$@PCNFs

Sample	Specific surface area, m^2 g^{-1}
PCNFs	1306
TiO2@PCNFs	1418

expansion of sulfur cathode during lithiation but also provide pathway for fast transport of electrons during cycling process. Furthermore, TiO$_2$ nanoparticles chemically adsorb

polysulfides owing to strong interaction between TiO$_2$ and polysulfides and hence leads to enhanced cycling performance with satisfactory reversible capacity.

XRD diffraction patterns of PCNFs and TiO$_2$@PCNFs are shown in Fig. 3. The peak at about 27^0 in the two curves demonstrated the existence of nongraphic carbon. The peak at 25^0 in the curve for TiO$_2$@PCNFs was the typical and strongest peak of rutile TiO$_2$ and all the identified peaks in the XRD pattern could be assigned to the rutile TiO$_2$ phase.[25] BET surface area measurement results of PCNFs and TiO$_2$@PCNFs were also reported in Table 1. The surface areas were 1306 m^2 g^{-1} and 1418 m^2 g^{-1} respectively, for PCNFs and TiO$_2$@PCNFs. The surface area of TiO$_2$@PCNFs was slightly increased compared to PCNFs owing to new surface contributed by the TiO$_2$ nano-particle deposition.

3.2 Electrochemical characteristics

Cycling voltammograms (CVs) of the Li–S cells with TiO$_2$@-PCNF interlayer, PCNF interlayer, and without interlayer are shown in Fig. 4. For all cells studied, in every cathodic scan, the peaks were observed at 2.3 V and 2 V, associated with the transformation of cyclo S to polysulfides (Li$_2$S$_x$, $4 \leq x \leq 8$) and reduction of polysulfides into Li$_2$S$_2$ and Li$_2$S, respectively.[5] Two anodic peaks were seen at around 2.3 V and 2.4 V where the insoluble LiS changed into polysulfides and then the element S. The CV of the Li–S cells with TiO$_2$@PCNF interlayer showed the highest current, indicating higher reversible capacity compared to the cell with PCNF interlayer and without interlayer. Zhuang *et al.*[6] prepared MoO$_2$ containing CNF interlayer and higher current observed from the CV curves of the cell with MoO$_2$/CNF
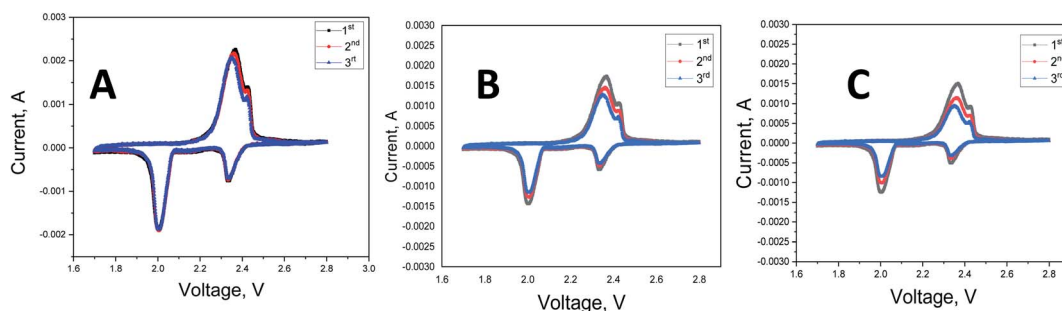

Fig. 4 Cyclic voltammograms of Li−S cells with TiO$_2$@PCNF interlayer (A), PCNF interlayer (B) and without interlayer (C).
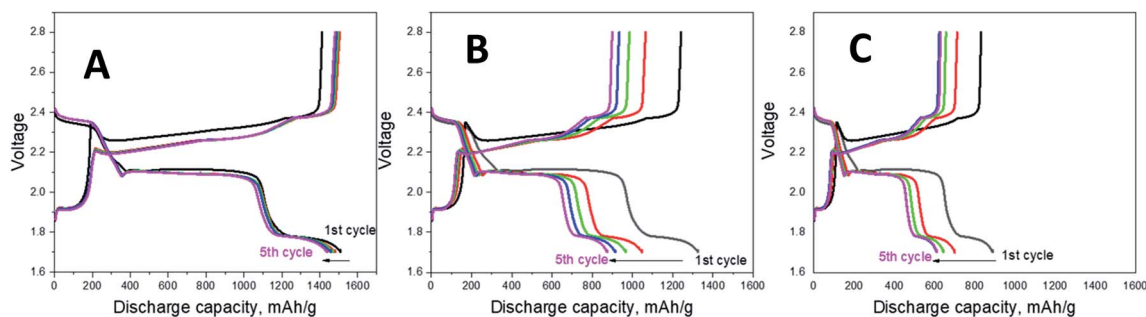

Fig. 5 Galvanostatic charge/discharge profiles of Li−S cells with TiO$_2$@PCNF interlayer (A), PCNF interlayer (B) and without interlayer (C).
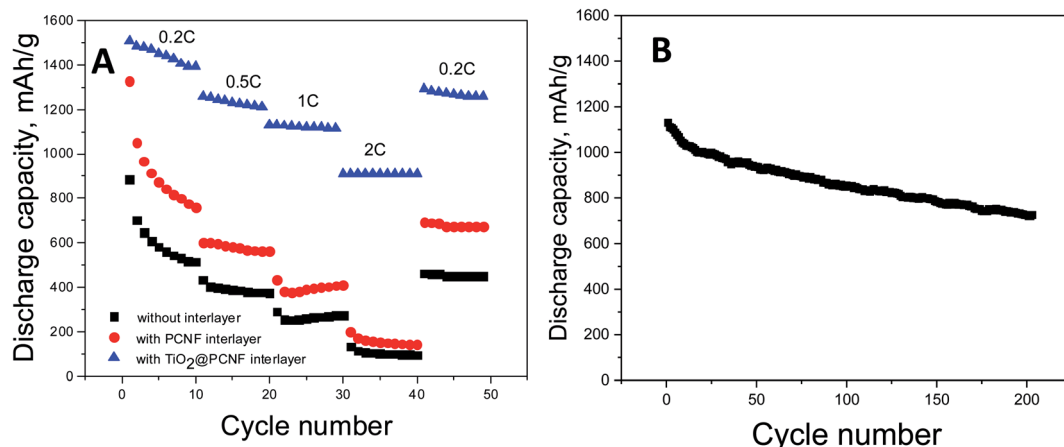
Fig. 6 C-rate performance of Li–S cells with TiO_2@PCNF interlayer, PCNF interlayer and without interlayer (A) cycling performance of Li–S cell with TiO_2@PCNF interlayer at 1C (B).

interlayer compared to that of the cell without interlayer, indicating better sulfur utilization due to strong polysulfide adsorption capacity of MoO_2/CNF interlayer.[6] Moreover, after the first cycle, no obvious change was observed, indicating superior electrochemical performance.

Fig. 5 shows the first cycle discharge–charge curves for the cells with TiO_2@PCNF interlayer, PCNF interlayer, and without interlayer. The typical two-plateau behavior of Li–S battery was observed at around 2.3 and 2.1 V, which was consisted with the peaks in the CV curves. The cell without interlayer delivered an initial discharge capacity of 884 mA h g^{-1}, meaning 52% utilization while the cells with TiO_2@PCNF interlayer and PCNF interlayer reached the discharge capacities of 1510 and 1326 mA h g^{-1}, corresponding to 90% and 79% utilization, respectively. The enhanced initial discharge capacity for the cells with TiO_2@PCNF interlayer was attributed to conductive nanostructured carbon network decorated with TiO_2 nanoparticles, in which PCNF provides excellent electron pathway while TiO_2 nanoparticles provide strong chemical adsorption for polysulfides.

The rate performance was measured at a stepwise current stage from 0.2C to 0.5C, to 1C, to 2C, and then back to 0.2C. When current changes to 0.2C to 0.5C, to 1C, to 2C, the cell with TiO_2@PCNF interlayer exhibited the discharge capacities of around 1400, 1200, 1150, and 900 mA h g^{-1} whereas the cell without interlayer delivered the capacities of 515, 375, 272 and 94 mA h g^{-1}.

Superior C rate performance illustrates that TiO_2@PCNF interlayer was effective for preventing shuttle of sulfur species. TiO_2 nanoparticles decorated on PCNFs can capture polysulfides effectively *via* the strong chemical adsorption resulting from the intense electrostatic attraction between the Ti–O bond and the sulfur species. Xiao *et al.*[5] introduced graphene/TiO_2 interlayer and they also reported enhanced C rate performance owing to low resistance, highly efficient entrapment of polysulfides and accommodated volume variations by using graphene/TiO_2 interlayer.[5] Cycling performance at 1C was also reported in Fig. 6 and discharge capacity of above 700 mA h g^{-1}

was achieved after 200 cycles which was significantly higher than that (around 400 mA h g^{-1}) of Li–S cells without interlayer.[17]

Fig. 7 shows the cycling stability for the cells with TiO_2@-PCNF interlayer, PCNF interlayer, and without interlayer. The cells with TiO_2@PCNF interlayer not only delivered the highest reversible capacity but also showed the highest capacity retention. In 200 cycles, the cell with TiO_2@PCNF interlayer delivered the high capacity of 968 mA h g^{-1} while the cells with PCNF interlayer and without interlayer only had the capacities of 498 and 206 mA h g^{-1}, respectively. The remarkable improvement could be attributed to improved electrical conductivity with nanostructured carbon network and strong adsorption of polysulfides with TiO_2 nanoparticles. Moreover carbon structure in the interlayer provided buffer like structure and reduced fracture in the cathode and provided conductive layer for re-using polysulfides. Jiao *et al.*[7] reported TiO/Mxene interlayer and
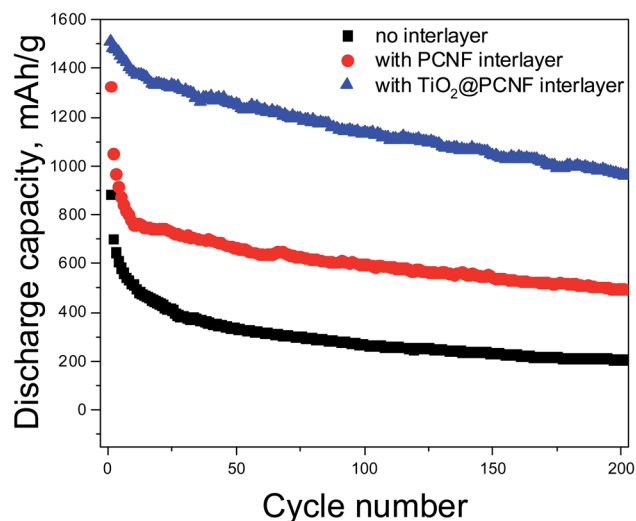

Fig. 7 Galvanostatic charge–discharge curves of Li–S cells with TiO_2@PCNF interlayer, PCNF interlayer and without interlayer.
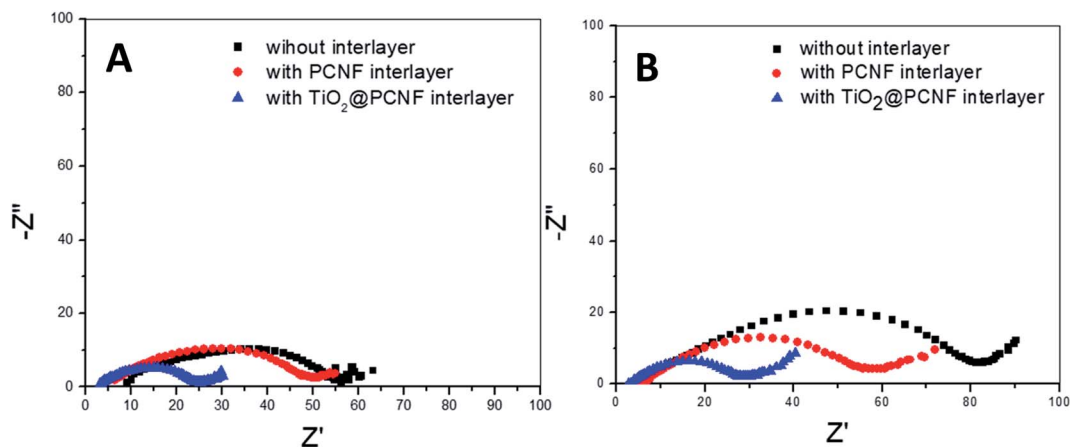
Fig. 8 Electrochemical impedance spectra of the Li–S cells with TiO_2@PCNF interlayer, PCNF interlayer and without interlayer before (A) and after (B) cycling.

better cycling performance with higher capacity (900 mA h g^{-1} compared to 600 mA h g^{-1} in 200 cycles) was attributed to strong polysulfide capturing ability of TiO_2.[7]

Electrochemical impedance spectroscopy of the cells before and after cycling is shown in Fig. 8. For all the cells studied, a semi-circle in the high to medium frequency region was observed, which is typical for Li–S cells. The semi-circle indicates the charge transfer resistance at the interface between the cathode and the electrolyte.[15] The charge transfer resistance of the cell with TiO_2@PCNF interlayer and PCNF interlayer was 25 and 50 ohm, respectively, whereas the cell without interlayer exhibited the charge transfer resistance of 55 ohm. The lower resistance of the cell with TiO_2@PCNF interlayer was attributed to conductive porous carbon network, which provides excellent electron pathway and thus leads to higher sulfur utilization. After cycling the resistance values were 30, 60 and 80 ohm for the cells with TiO_2@PCNF interlayer, PCNF interlayer, and without interlayer, respectively, indicating the formation of an insulating layer of solid Li_2S_2/Li_2S between the separator and the cathode.[25] After 200 cycles, the cell with TiO_2@PCNF interlayer, showed the lowest resistance due to the sufficient infiltration of the electrolyte to the interlayer and the sulfur cathode, indicating that TiO_2@PCNF interlayer restricted polysulfide shuttling, supported lithium ion movement and thus leading to lower resistance with superior cycling and C rate performance. All these results proves that TiO_2@PCNF interlayer was effective in prohibiting the shuttle effect of polysulfides in Li–S batteries.

4. Conclusion

A facile and effective way to fabricate TiO_2 decorated PCNF interlayer was developed for Li–S batteries. The enhanced cycling and C rate performance was achieved. The conductive PCNF network provided excellent electron pathway, and thus improved electron transfer and help reutilization of active material while TiO_2 nanoparticles adsorbed polysulfides effectively through strong chemical adsorption. This study reported one step feasible approach to fabricate conductive interlayer

with highly adsorbent nanoparticles and tunable properties to improve electrochemical performance of Li–S batteries without electrode modification. This novel porous and conductive structure not only adsorb polysulfides but also help reutilization of the active material on the cathode side. The findings in this work reveal a scalable and effective method to fabricate interlayers that could provide remarkable development for Li–S batteries.

Conflicts of interest

The authors declare that they have no conflict of interest.

References

1 H. Xiang, J. Chen, Z. Li, *et al.*, An inorganic membrane as a separator for lithium-ion battery, *J. Power Sources*, 2011, **196**, 8651–8655.

2 X. Chen, W. He, L.-X. Ding, *et al.*, Enhancing interfacial contact in all solid state batteries with a cathode-supported solid electrolyte membrane framework, *Energy Environ. Sci.*, 2019, **12**, 938–944.

3 Z. Jiang, H. Xie, S. Wang, *et al.*, Perovskite Membranes with Vertically Aligned Microchannels for All-Solid-State Lithium Batteries, *Adv. Energy Mater.*, 2018, **8**, 1801433.

4 C. Ye, Y. Jiao, D. Chao, *et al.*, Electron-State Confinement of Polysulfides for Highly Stable Sodium–Sulfur Batteries, *Adv. Mater.*, 2020, 1907557.

5 Z. Xiao, Z. Yang, L. Wang, *et al.*, A lightweight TiO2/graphene interlayer, applied as a highly effective polysulfide absorbent for fast, long-life lithium–sulfur batteries, *Adv. Mater.*, 2015, **27**, 2891–2898.

6 R. Zhuang, S. Yao, X. Shen, *et al.*, A freestanding MoO2-decorated carbon nanofibers interlayer for rechargeable lithium sulfur battery, *Int. J. Energy Res.*, 2019, **43**, 1111–1120.

7 L. Jiao, C. Zhang, C. Geng, *et al.*, Capture and Catalytic Conversion of Polysulfides by In Situ Built TiO2-MXene

Heterostructures for Lithium–Sulfur Batteries, *Adv. Energy Mater.*, 2019, **9**, 1900219.

8 B. Q. Li, L. Kong, C. X. Zhao, *et al.*, Expediting redox kinetics of sulfur species by atomic-scale electrocatalysts in lithium–sulfur batteries, *Infomatics*, 2019, **1**, 533–541.

9 W. Chen, Y. Hu, W. Lv, *et al.*, Lithiophilic montmorillonite serves as lithium ion reservoir to facilitate uniform lithium deposition, *Nat. Commun.*, 2019, **10**, 1–9.

10 J. Y. Hwang, H. M. Kim, S. K. Lee, *et al.*, High-Energy, High-Rate, Lithium–Sulfur Batteries: Synergetic Effect of Hollow TiO2-Webbed Carbon Nanotubes and a Dual Functional Carbon-Paper Interlayer, *Adv. Energy Mater.*, 2016, **6**, 1501480.

11 X. T. Gao, Y. Xie, X. D. Zhu, *et al.*, Ultrathin MXene nanosheets decorated with TiO2 quantum dots as an efficient sulfur host toward fast and stable Li–S batteries, *Small*, 2018, **14**, 1802443.

12 D.-R. Deng, T.-H. An, Y.-J. Li, *et al.*, Hollow porous titanium nitride tubes as a cathode electrode for extremely stable Li–S batteries, *J. Mater. Chem. A*, 2016, **4**, 16184–16190.

13 C. Gao, C. Fang, H. Zhao, *et al.*, Rational design of multi-functional CoS@ rGO composite for performance enhanced Li-S cathode, *J. Power Sources*, 2019, **421**, 132–138.

14 J. He, Y. Chen, W. Lv, *et al.*, Three-dimensional CNT/graphene–Li2S aerogel as freestanding cathode for high-performance Li–S batteries, *ACS Energy Lett.*, 2016, **1**, 820–826.

15 Y. Liu, X. Qin, S. Zhang, *et al.*, Fe3O4-Decorated Porous Graphene Interlayer for High-Performance Lithium–Sulfur Batteries, *ACS Appl. Mater. Interfaces*, 2018, **10**, 26264–26273.

16 T. Lei, W. Chen, W. Lv, *et al.*, Inhibiting polysulfide shuttling with a graphene composite separator for highly robust lithium-sulfur batteries, *Joule*, 2018, **2**, 2091–2104.

17 T. Lei, W. Chen, Y. Hu, *et al.*, A Nonflammable and Thermotolerant Separator Suppresses Polysulfide Dissolution for Safe and Long-Cycle Lithium-Sulfur Batteries, *Adv. Energy Mater.*, 2018, **8**, 1802441.

18 W. Chen, T. Lei, W. Lv, *et al.*, Atomic interlamellar ion path in high sulfur content lithium-montmorillonite host enables high-rate and stable lithium–sulfur battery, *Adv. Mater.*, 2018, **30**, 1804084.

19 T. Lei, Y. Hu, W. Chen, *et al.*, Genetic engineering of porous sulfur species with molecular target prevents host passivation in lithium sulfur batteries, *Energy Storage Materials*, 2020, **26**, 65–72.

20 S. Li, G. Ren, M. N. F. Hoque, *et al.*, Carbonized cellulose paper as an effective interlayer in lithium-sulfur batteries, *Appl. Surf. Sci.*, 2017, **396**, 637–643.

21 C. Zu, Y.-S. Su, Y. Fu, *et al.*, Improved lithium–sulfur cells with a treated carbon paper interlayer, *Phys. Chem. Chem. Phys.*, 2013, **15**, 2291–2297.

22 K. Zhang, Q. Li, L. Zhang, *et al.*, From filter paper to carbon paper and toward Li–S battery interlayer, *Mater. Lett.*, 2014, **121**, 198–201.

23 Y.-S. Su and A. Manthiram, Lithium–sulphur batteries with a microporous carbon paper as a bifunctional interlayer, *Nat. Commun.*, 2012, **3**, 1–6.

24 Y. Yang, W. Sun, J. Zhang, *et al.*, High rate and stable cycling of lithium-sulfur batteries with carbon fiber cloth interlayer, *Electrochim. Acta*, 2016, **209**, 691–699.

25 N. Li, Z. Chen, F. Chen, *et al.*, From interlayer to lightweight capping layer: Rational design of mesoporous TiO2 threaded with CNTs for advanced Li–S batteries, *Carbon*, 2019, **143**, 523–530.

26 P. Huang and Y. Wang, Carpet-like TiO2 Nanofiber Interlayer as Advanced Absorber for High Performance Li-S batteries, *Int. J. Electrochem. Sci.*, 2019, **14**, 5154–5160.